Supplementary Information

An aggregation-induced emission-active theranostic agent for selectively detecting and intervening pathological Tau protein

Jixue Yang,[a] Youwen Deng,[a] Shu Qin,[a] Ziting Chen,[a] Yuting Lu,[a] Shunli Ji,[a] Taijun Hang,[a] and Min Song*[a]

[a.] *Department of Pharmaceutical Analysis, China Pharmaceutical University, Nanjing 210009, China. E-mail: songmin@cpu.edu.cn*

EXPERIMENTAL METHODS

Materials

Peptide (CKVQIINKK) was custom-synthesized by BankPeptide Biological Technology Co., Ltd. (Hefei, China). Recombinant human Tau protein (2N4R) was supplied by HuaBio (Hangzhou, China). Recombinant human glycogen synthase kinase-3β (GSK3β) was obtained from SinoBiological (Beijing, China). Heparin was purchased from Shanghai Yuanye Bio-Technology Co., Ltd. (Shanghai, China). Thioflavin T (ThT), and 1,1',1",1"'-(1,2-ethenediylidene)-tetrakisbenzene (TPE) were supplied by Macklin Biochemical Co., Ltd. (Shanghai, China). 4-(1,2,2-triphenylvinyl)aniline (TPE-NH_2) was purchased from Bide Pharmatech Co., Ltd. (Shanghai, China). Okadaic acid (OA) was supplied by Amgicam (Shanghai, China). Protein marker (10-250 kDa) was acquired from Thermo Fisher Scientific (Waltham, United States). Precast PAGE gel (4-20%) and SDS-PAGE protein loading buffer (5×) were supplied by Beyotime Institute of Biotechnology (Shanghai, China). Polyclonal anti-Tau antibody and HRP-conjugated affinipure goat anti-rabbit IgG (H+L) were purchased from Proteintech (Wuhan, China). Monoclonal anti-Tau (phospho S396) antibody was obtained from Abcam (Cambridge, United Kingdom). Ultrapure water (18.25 MΩ cm^{-1}) was purified with a Milli Q-Plus purification system (Bedford, MA, United States). All other chemicals and reagents were procured from commercial suppliers and utilized without additional purification.

Instrumentations

^{1}H, ^{13}C, DEPT, ^{1}H-^{1}H COSY, HSQC, and HMBC nuclear magnetic resonance (NMR) spectra were recorded on a Bruker Avance AV-500 spectrometer (Germany). Primary and secondary mass spectra were measured on Shimadzu LC–MS-9030 quadrupole/time-of-flight (Q-TOF) mass spectrometer (Japan). All the fluorescence determinations were carried out on a Shimadzu RF-5301 spectrophotometer. CCK-8 assay was recorded on a SpectraMax CMax Plus absorbance reader (United States). Western blot (WB) images were obtained from Tanon 4600 automatic chemiluminescence image analysis system (China).

Preparation of the Probe

1-(4-(1,2,2-triphenylvinyl)phenyl)-1H-pyrrole-2,5-dione (TPE-Mal) was prepared according to the procedure previously reported with some modifications.[1] Briefly, TPE-NH_2 and maleic anhydride were mixed and stirred at room temperature, followed by the addition of sodium acetate and acetic anhydride, and stirring at 90 ℃ for another 3 h. The resultant solution was poured into ice-cold water and extracted three times with dichloromethane. The organic layer was washed, dried over anhydrous sodium sulfate, and concentrated under vacuum, with the crude product purified by silica gel column chromatography. ^{1}H-NMR (500 MHz, DMSO-d_6) δ (ppm) = 7.20-6.97 (m, 21H). ^{13}C-NMR (125 MHz, DMSO-d_6) δ (ppm) = 170.29, 143.53, 143.50, 143.45 142.81, 141.60, 140.25, 135.12, 131.45, 131.14, 131.09, 130.21, 128.45, 128.40, 128.31, 127.24, 127.14, 127.10, 126.22. HRMS (ESI) *m/z*: $[M+H+MeOH]^+$ calcd for $C_{31}H_{26}NO_3$, 460.1907; found, 460.2038. $[M+Na+MeOH]^+$ calcd for $C_{31}H_{25}NO_3Na$, 482.1727; found, 482.1916. $[M+K+MeOH]^+$ calcd for $C_{31}H_{25}NO_3K$, 498.1466; found, 498.1594.

The peptide-AIEgen conjugate (TPE-P9) was synthesized by Michael reaction between the thiol group of the peptide (CKVQIINKK) and the maleimide group of TPE-Mal under ambient conditions. The resulting product was purified by high-performance preparative liquid chromatography and subsequently lyophilized for further use.

Investigations on Photophysical Properties of Probes

To investigate the aggregation-induced emission (AIE) properties of the probes, TPE, TPE-P9, and ThT were initially dissolved in DMF (a good solvent) to prepare stock solutions. These solutions were then diluted with either water (a poor solvent for TPE and TPE-P9) or tetrahydrofuran (a poor solvent for ThT) to achieve a final concentration of 10 μM. The emission spectra of the probes were recorded using a fluorescence spectrophotometer with excitation wavelengths of 320 nm for TPE, 330 nm for TPE-P9, and 385 nm for ThT.

Preparations of Tau, p-Tau, and $A\beta_{1-42}$ Aggregates in Vitro

2 $mg \cdot mL^{-1}$ recombinant human Tau protein (2N4R) was prepared in a buffer containing 20 mM Tris-HCl, and 100 mM NaCl at pH 7.4, supplemented with 1 mM DTT and incubated at 37 °C for 2 h prior to the aggregation reactions to reduce any covalent linkage inter- or intra- Tau molecules. The reactions were initiated with addition of oligomerization inducer, heparin, at the final concentration to 10 μM, followed by incubation at 37 °C without agitation for different time.

The p-Tau protein was prepared by incubating 2 $mg \cdot mL^{-1}$ Tau with 0.118 $mg \cdot mL^{-1}$ GSK3β in a buffer containing 20 mM Tris-HCl, 150 mM NaCl, 20 mM $MgCl_2$, and 5 mM DTT at pH 7.4. The kinase reactions were initiated by addition of 3 mM ATP and followed by incubating at 37 °C without agitation for different time. Then the buffer was replaced with the aggregation buffer containing 20 mM Tris-HCl, and 100 mM NaCl at 4 °C through ultrafiltration to stop the reaction.

A total of 1 mg of freeze-dried $A\beta_{1-42}$ peptide powder was dissolved in 1 mL of 1,1,1,3,3,3-hexafluor-2-popanol (HFIP) and incubated at room temperature for 2 h to breakdown pre-existing aggregates, then the solvent was removed by nitrogen flow. The monomeric peptide solutions were prepared by addition of 100 μL of DMSO to HFIP-treated $A\beta_{1-42}$, followed by dilution with a buffer containing 20 mM Tris-HCl, and 100 mM NaCl at pH 7.4, then the solutions were sonicated in ice-water bath for 10 min and subsequently centrifugation at 14000 rpm at 4 °C for 15 min. The supernatants were collected as monomers. The aggregation reactions of $A\beta_{1-42}$ were performed by incubating monomeric peptide solutions at 37 °C without agitation for different time.

Transmission Electron Microscopy (TEM) Measurement

Tau monomers were incubated at 37 ℃ to induce fibrillar aggregation. The original samples were diluted four times. TEM images were acquired using a Hitachi HT7800 electron microscope (Japan) operated at 80 kV. For each sample, 10 μL of protein solution was blotted onto a copper grid with a formvar coating for 1 min. The samples were then stained with 2.0% phosphotungstic acid for 1 min and observed under magnifications ranging from 10,000x to 50,000x.

Fluorescence Analysis in Solution

The Tau protein or $A\beta_{1-42}$ peptide was incubated for a defined period of time. The obtained monomers and fibrils were diluted to appropriate concentrations, followed by supplementation with the dye (ThT or TPE-P9) to a final concentration of 1 μM. After incubation at 37 ℃ for 10 min, the fluorescence intensities were recorded at 485 nm for ThT and 465 nm for TPE-P9, with excitation wavelengths at 440 nm and 330 nm, respectively. Each experiment was independently repeated at least three times.

Microscale Thermophoresis (MST) Measurement

Monomeric Tau (2N4R) protein (1 $mg \cdot mL^{-1}$, 10 mM HEPES, 100 mM NaCl, pH 7.4) was prepared by buffer replacement through ultrafiltration. Abnormal Tau was prepared according to reported procedures.[29] Proteins were labeled using the RED-tris-NTA 2nd Generation protein labeling kit (Nanotemper). Subsequently, normal Tau or abnormal Tau was incubated with TPE-P9 or ThT for binding affinity testing at room temperature. The affinity constant (K_d) of TPE-P9 and ThT with normal Tau or abnormal Tau was measured using the Monolith NT.115 instrument (Nanotemper), and the obtained data were analyzed using MO. Affinity Analysis *v*2.3 software.

Fluorescence Imaging in Living Cells

HT22 cells were cultured in 24-well plates until adhered to the surface. Then, the cells were co-incubated with 100 nM of OA for another 12 h to induce p-Tau. Afterward, the media were replaced with 20 μM of TPE-P9 or ThT, and incubated in dark for 30 min. Cells were washed in PBS buffer for three times to remove excess probes and dead cells. The fluorescence images were captured using an inverted fluorescence microscope (Nikon Eclipse Ti2), with band pass excitation filters were 340-400 nm for TPE-P9 and 430-465 nm for ThT. the obtained data were analyzed using NIH ImageJ *v*1.54h software.

Co-localization Imaging of TPE-P9 with Anti-p-Tau Antibody

HT22 cells were seeded in 12-well plates containing glass coverslips and cultured until complete adherence. To induce Tau hyperphosphorylation, cells were treated with 100

nM OA for 12 hours. After induction, the culture medium was aspirated, and cells were fixed with pre-chilled methanol for 15 min. Permeabilization was performed by incubating cells in PBS supplemented with 0.5% Triton X-100 for 20 min, followed by blocking with 5% BSA for 60 min at room temperature. For immunolabeling, cells were incubated overnight at 4 °C with a primary anti-p-Tau (48856, CST, 1:100) antibody. After three washes with PBS, coverslips were incubated with a fluorescently conjugated secondary antibody (RGAR004, Proteintech, 1:200) for 1 h at room temperature in the dark. Subsequently, cells were stained with 20 μM TPE-P9 for 30 min. Coverslips were mounted onto glass slides using anti-fade mounting medium (P0126-25ml, Beyotime) to minimize fluorescence quenching. Fluorescence images were acquired using an inverted fluorescence microscope (Nikon Eclipse Ti2) with excitation filters set to 340–400 nm for TPE-P9 and 510–560 nm for anti-p-Tau antibody detection, respectively.

Effects of Okadaic Acid (OA) on Tau Hyperphosphorylation

HT22 cells were pre-treated with or without OA for 12 h. Then proteins were extracted from the cells using ice-cold RIPA lysis buffer (Beyotime), supplemented with protease and phosphatase inhibitors (Beyotime). Protein concentrations were determined using a BCA protein assay kit (Beyotime). The extracted proteins were stored at -80 °C for subsequent analysis. The levels of both total Tau and p-Tau were semi-quantified by WB.

Western Blot Analysis

Tau proteins were pre-treated with 5× SDS-PAGE loading buffer. For each sample, an equal amount of protein was subjected to SDS-PAGE on precast 4%-20% gels and then transferred onto PVDF membranes (Millipore, Bedford, MA, USA). The membranes were blocked with 5% BSA for 1.5 h at room temperature, followed by incubation with primary anti-Tau (10274-1-AP, Proteintech, 1:3000), anti-p-Tau (ab109390, Abcam, 1:20000) or anti-GADPH (60004-1-1g, Proteintech, 1:20000) antibodies at 4 °C overnight. After washing three times with TBST, the membranes were incubated with corresponding secondary antibodies (Proteintech, 1:3000) for 1 h at room temperature. Immunoreactive bands were detected by developing with ECL luminescence reagent. The band intensities were quantified using NIH ImageJ *v*1.54h software.

Atomic Force Microscopy (AFM) Measurement

The morphological alterations of amyloid protein were meticulously characterized utilizing Bruker Dimension Icon atomic force microscope (Germany). Prior to analysis, samples were diluted in sterile water to appropriate concentrations. Subsequently, 10 μL of each sample was dropped onto a mica substrate. The samples were finally subjected to a drying process in air gas before use. The resulting images were analyzed using NanoScope Analysis *v*2.0 software.

Study of Amyloid Properties of TPE-P9

0.5 mg of TPE-P9 was dissolved in DMF to obtain stock solutions. Then, the samples were diluted in a Tris-HCl buffer at pH 7.4 on ice to reach final concentrations ranging from 1 μM to 60 μM, supplemented with 10 μM ThT as an aggregation indicator. The aggregation reactions were initiated at 37 ℃, and fluorescence intensities were subsequently recorded after incubation periods ranging from 1 to 96 hours. Each experiment was independently repeated at least three times.

Effects of TPE-P9 on Heparin or Hyperphosphorylated Induced Tau Aggregation

An appropriated amount of monomeric Tau was pre-incubated with TPE-P9 in different molar ratios of 10:1, 1:1, 1:5, and 1:10 (Tau:TPE-P9) for 1 h before addition of heparin or GSK3β acting as aggregates inducer or protein kinase. The reactions carried out at 37 °C for another 16 h for heparin-induced Tau oligomerization, and 72 h for GSK3β-induced Tau phosphorylation. Samples were diluted with 5× loading buffer and boiled for 10 min. The levels of Tau monomers were semi-quantified by WB.

Cell Culture

Mouse hippocampal neuron cells HT22 (Procell, Wuhan, China) were cultured in Dulbecco's modified Eagle's medium (DMEM; Keygen Biotech, Nanjing, China) supplemented with 10% fetal bovine serum (FBS; Bioind, Israel), 80 $U \cdot mL^{-1}$ penicillin, and 0.08 $mg \cdot mL^{-1}$ streptomycin (Keygen Biotech, Nanjing, China). All cells were propagated in T-75 flasks maintained in a humidified incubator with 5% (*v/v*) CO_2 at 37°C until the cell density reached approximately 80%.

Cell Viability Assay

Cell viability was assessed using a standard 2-(2-methoxy-4-nitrophenyl)-3-(4-nitrophenyl)-5-(2,4-disulfophenyl)-2*H*-tetrazolium sodium salt (CCK-8) reduction assay. Cells were seeded in 96-well plates (5×10^3 cells per well) and incubated at 37 ℃ for 24 h. For TPE-P9 cytotoxicity assessment, various concentrations of TPE-Mal, P9, and TPE-P9 (1-20 μM) were added and co-incubated with the cells for an additional 48 h. To evaluate the impact of TPE-P9 on endogenous hyperphosphorylated Tau (p-Tau)-induced apoptosis, the original media were replaced with OA/TPE-P9-OA solutions and cultured for another 12 h. Additionally, regarding the influence of TPE-P9 on exogenous Tau oligomer-induced cell death, heparin-Tau/p-Tau/TPE-P9-heparin-Tau/TPE-P9-p-Tau were supplemented and incubated for another 48 h. Subsequently, the medium was removed, and equal volumes of 10% CCK-8 culture medium solutions were added. The absorbance values were read at 450 nm after incubation at 37 ℃ for 30 min, and cell viability was determined as the percentage of CCK-8 reduction compared to untreated cells. Each experiment was independently repeated at least three times.

Cell Apoptosis Detecting by Flow Cytometry

p-Tau was prepared by incubating Tau with GSK3β in the abscence or presence of TPE-P9 at a molar ratio of 2:1 (TPE-P9:Tau) for 72 h. HT22 cells were cultured in 12-well plates until adhered to the surface. The medium was then replaced with solutions containing 5 μM of either native Tau, p-Tau (without TPE-P9), or TPE-P9 pretreated p-Tau (TPE-P9-p-Tau). Cells were further incubated for another 48 h. Subsequently, the original medium was aspirated, and cells were washed with PBS buffer for three times. Then, cells were resuspended in binding buffer following trypsin digestion. Finally, cells were stained with Annexin V-FITC/PI Apoptosis Detection Kit (A211-01, Vazyme) for 10 min at room temperature in the dark. Stained cell suspensions were diluted with additional binding buffer and filtered through a 48 μm mesh filter. Cytotoxicity induced by pathological Tau was quantified using a flow cytometer (BD FACS Celesta), with Annexin V-FITC and PI signals used to distinguish apoptotic and necrotic cells.

Evaluation of Pathological Tau Internalization by Flow Cytometry

Tau protein was labeled using HOOK^{TM} dye labeling kit (FITC) according to the manufacture's instructions. HT22 cells were cultured in 12-well plates until adhered to the surface. The medium was then replaced with solutions of Tau-FITC-heparin-TPE-P9 and the cells were incubated for another 16 h. Subsequently, the original medium was discarded and the cells were washed with PBS buffer for three times. Finally, cells were resuspended in PBS buffer following trypsin digestion. The internalization of the pathological Tau was quantified using a flow cytometer (BD FACS Celesta) and the obtained data were analyzed using FlowJo *v*10.10.0 software.

RESULTS

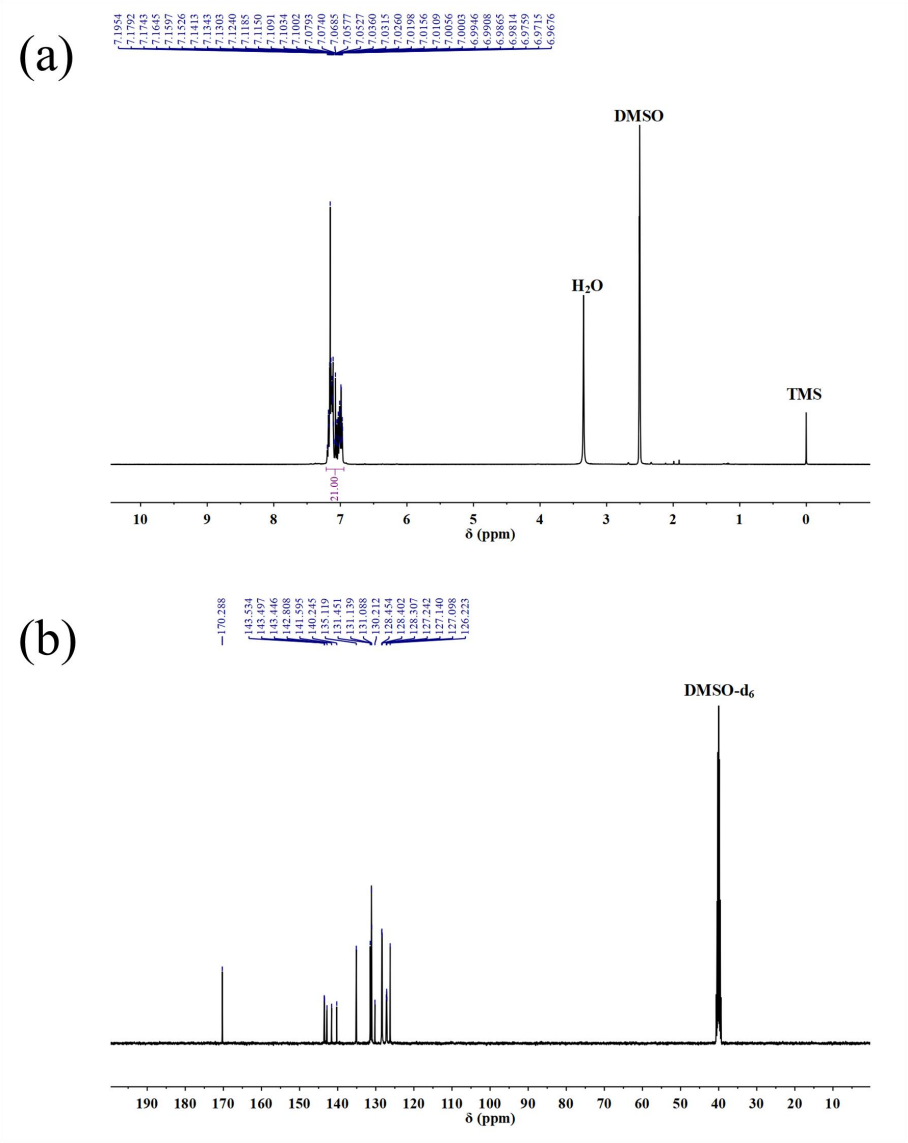

Fig. S1 *(*a) ^{1}H-NMR spectra of TPE-Mal in DMSO-d_6. (b) ^{13}C-NMR spectra of TPE-Mal in DMSO-d_6.

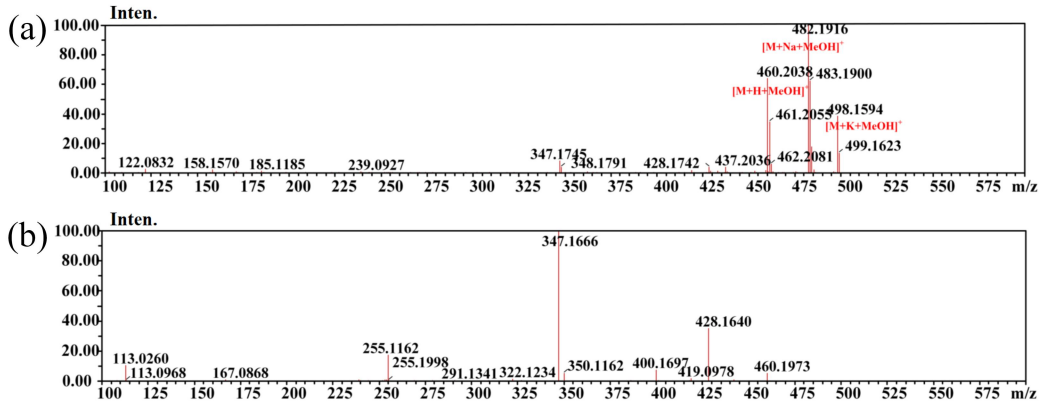

Fig. S2 The (a) primary and (b) secondary mass spectra of TPE-Mal.

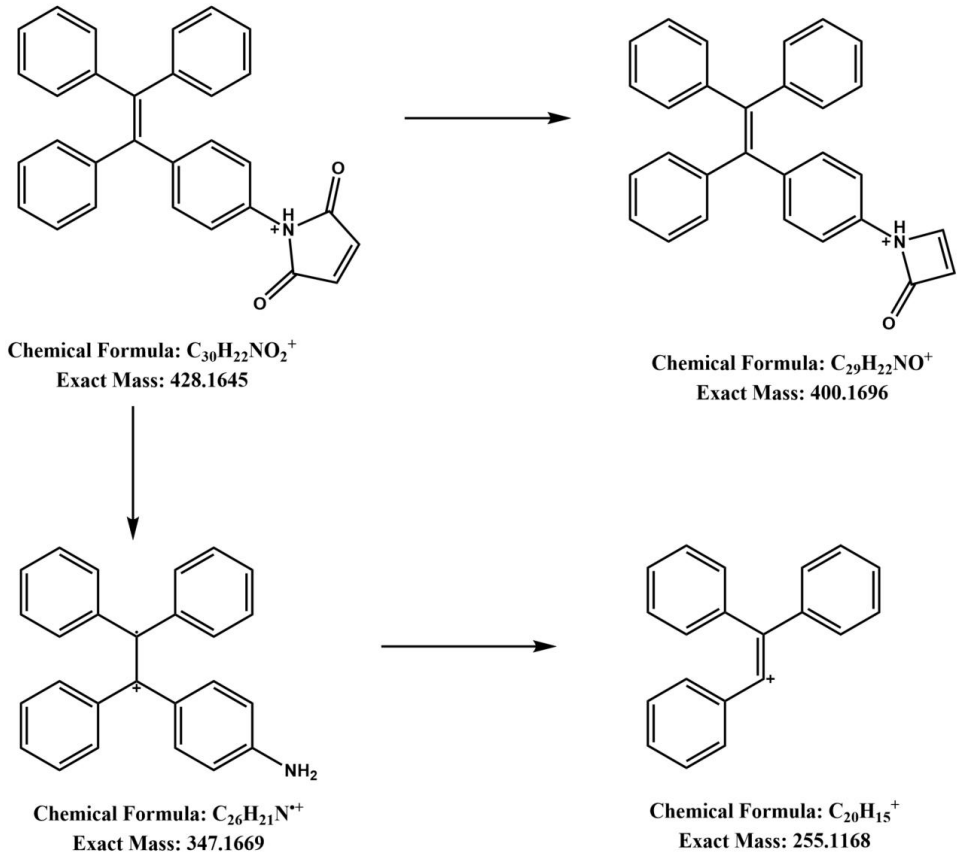

Fig. S3 Plausible fragmentation pathways of TPE-Mal in positive ion mode.

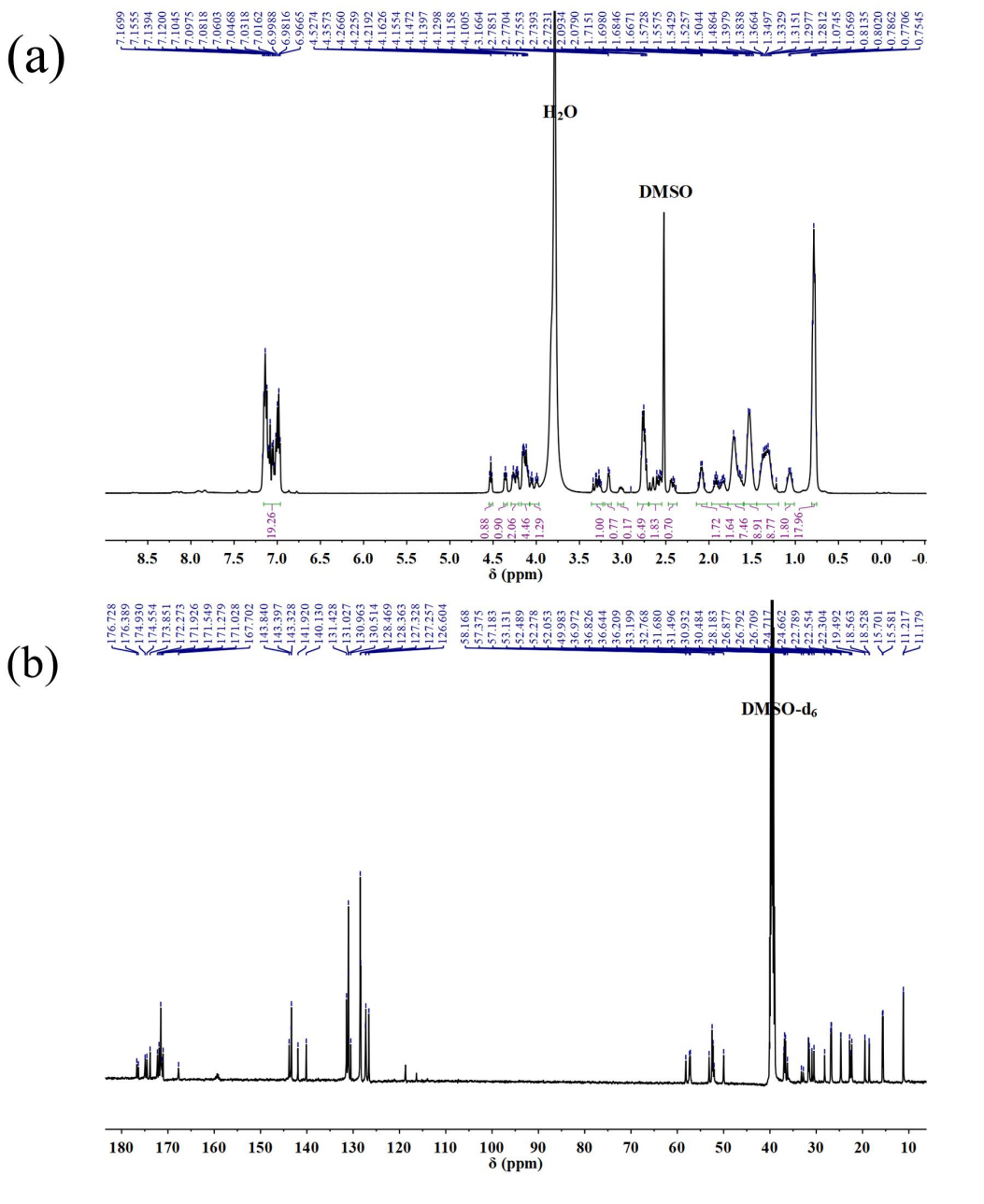
(a)
H2O
DMSO
δ (ppm)
(b)
DMSO-d6
δ (ppm)

(c)

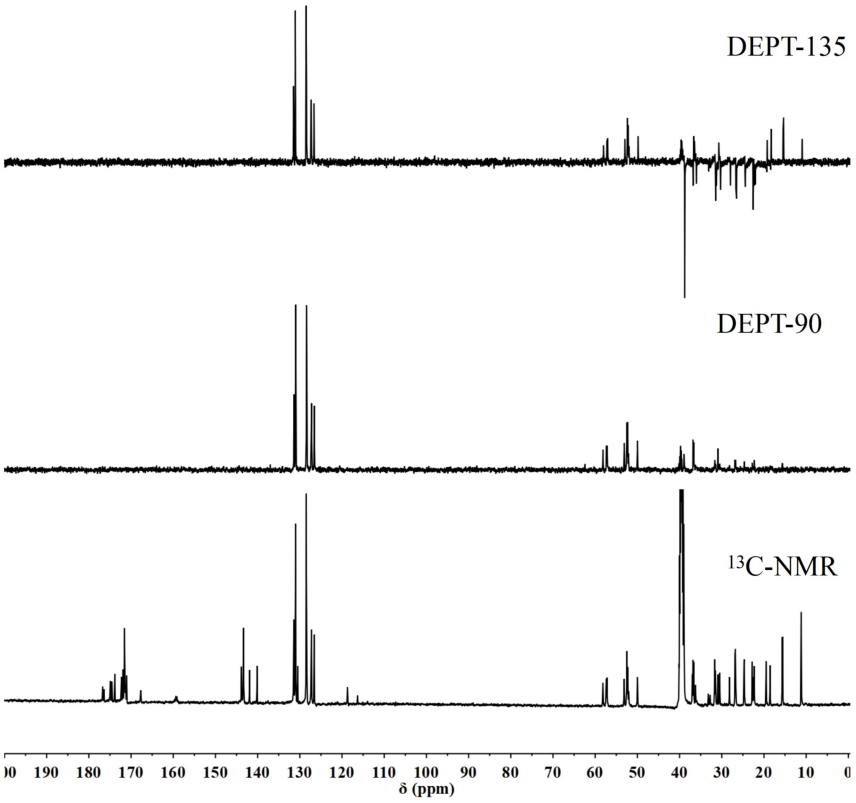

(d)

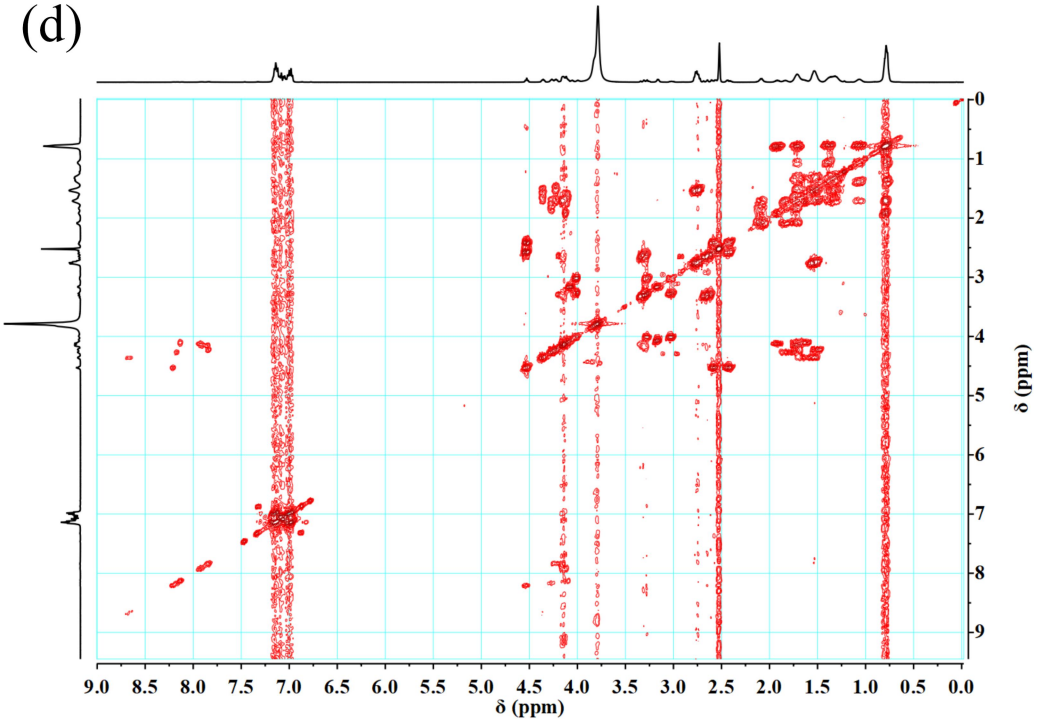

(e)

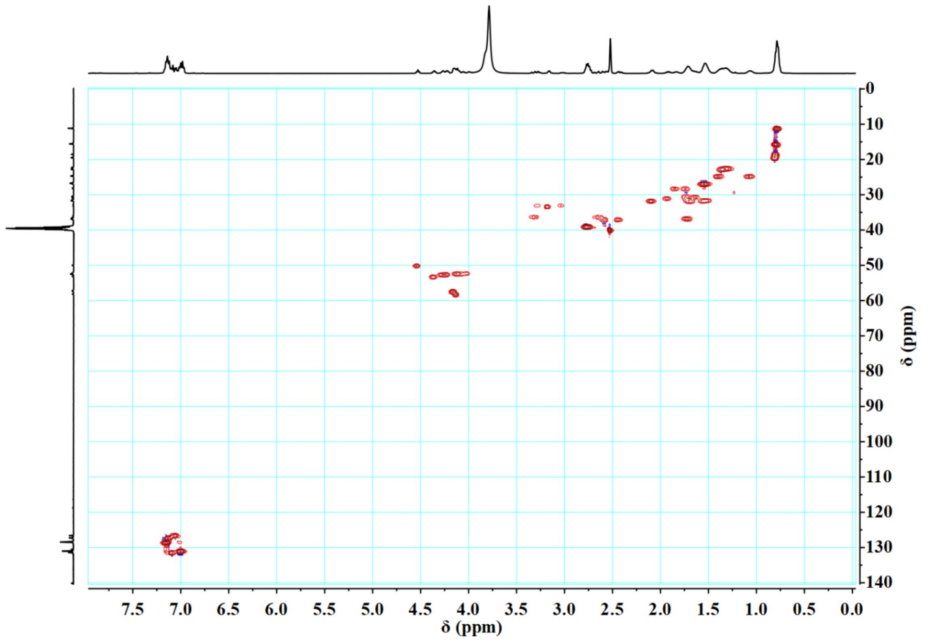

(f)

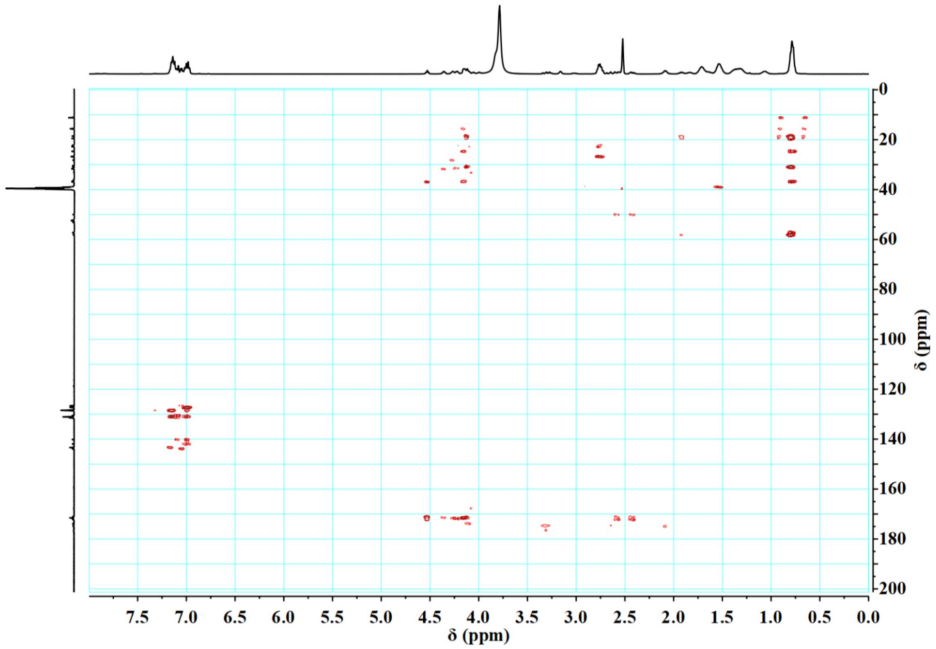

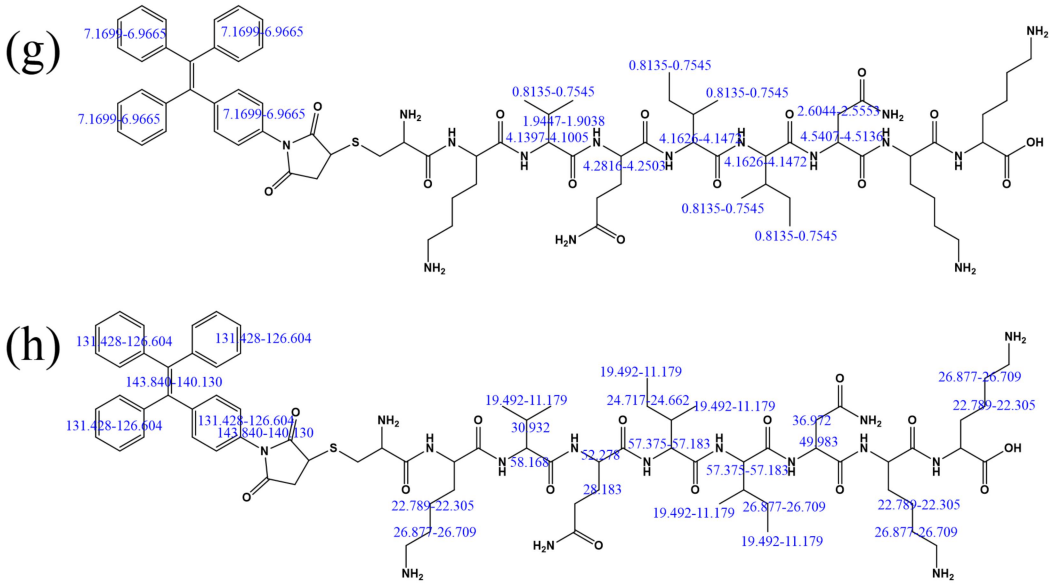

Fig. S4 (a) ^{1}H-NMR spectra, (b) ^{13}C-NMR spectra, (c) DEPT spectra, (d)^{1}H-^{1}H COSY spectra, (e) HSQC spectra, and (f) HMBC spectra of TPE-P9 in DMSO-d_6 and D_2O mixed solution. Corresponding chemical shift labeling of (g) hydrogen nucleus and (h) carbon nucleus based on the NMR spectra.

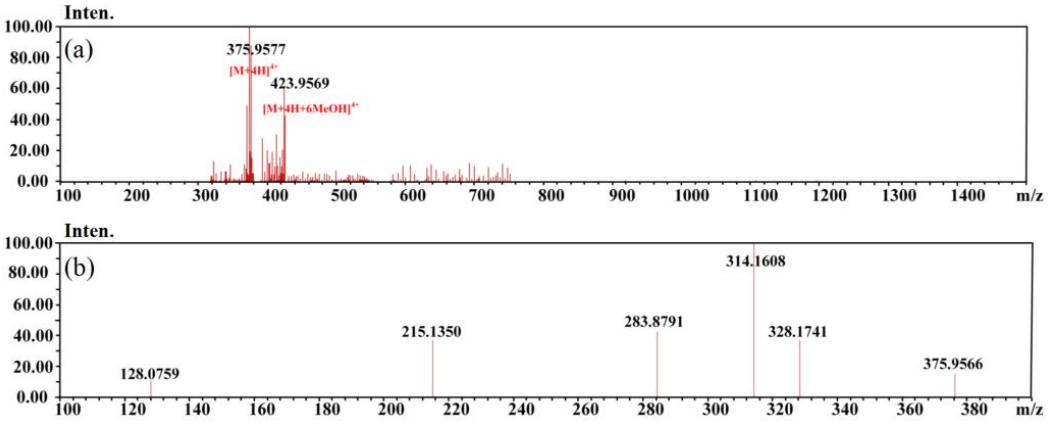

Fig. S5 The (a) primary and (b) secondary mass spectra of TPE-P9.

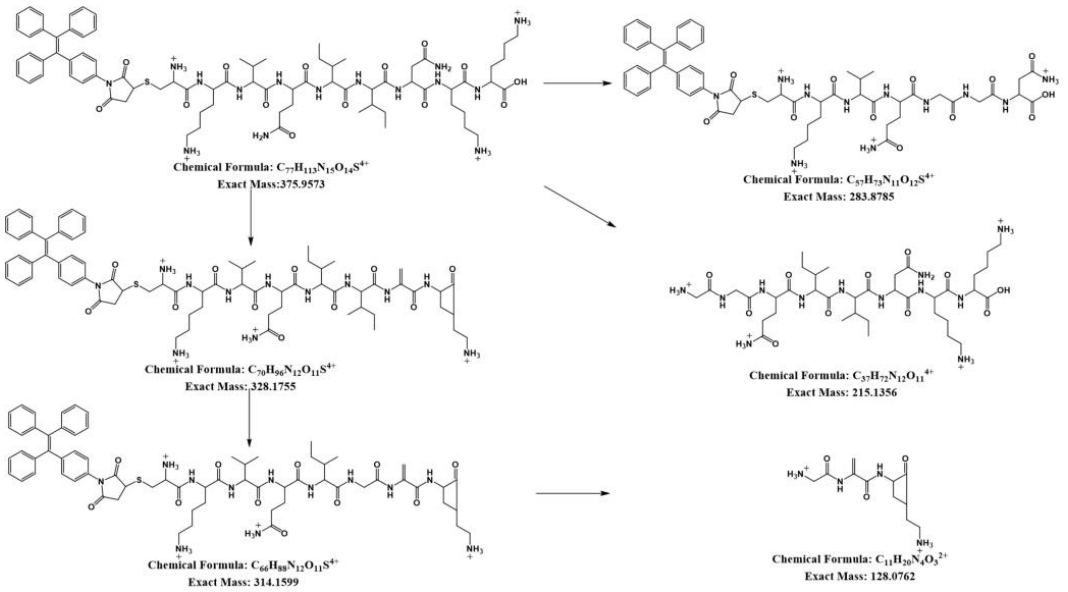

Fig. S6 Plausible fragmentation pathways of TPE-P9 in positive ion mode.

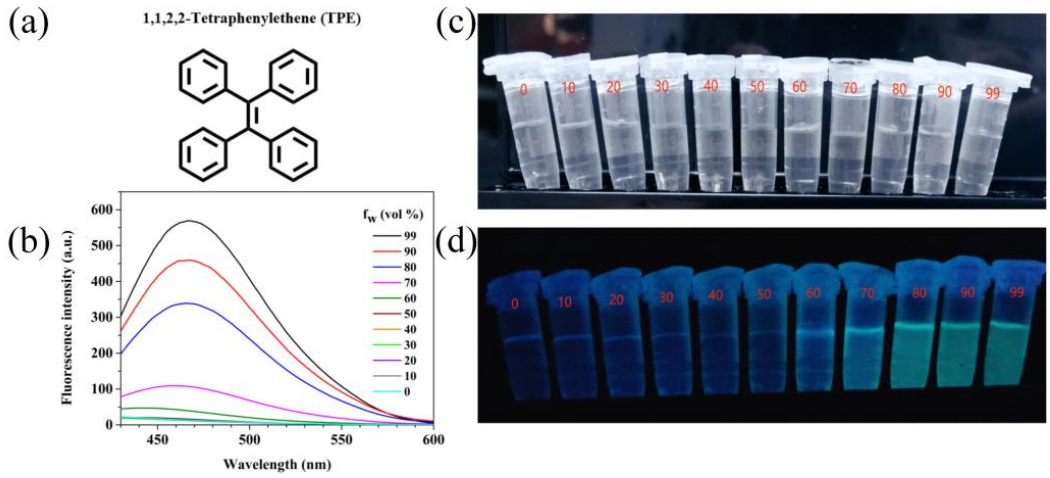

Fig. S7 AIE properties of TPE. (a) The chemical structure of TPE. (b) Emission spectra of TPE in a mixture of H_2O-DMF with different water fractions (f_w, vol.%), λ_{ex} = 320 nm. Photographs of 10 μM TPE with different water ratios of H_2O-DMF taken under (c) normal laboratory lighting and (d) irradiation with a UV light of 365 nm.

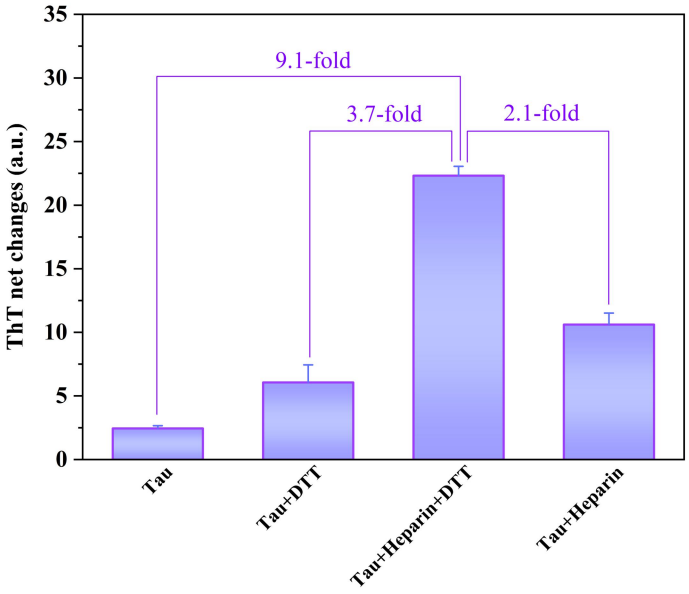

Fig. S8 Inducer-dependent and antioxidant-dependent fibrillization of Tau441 protein (4 μM) monitored by ThT (10 μM).

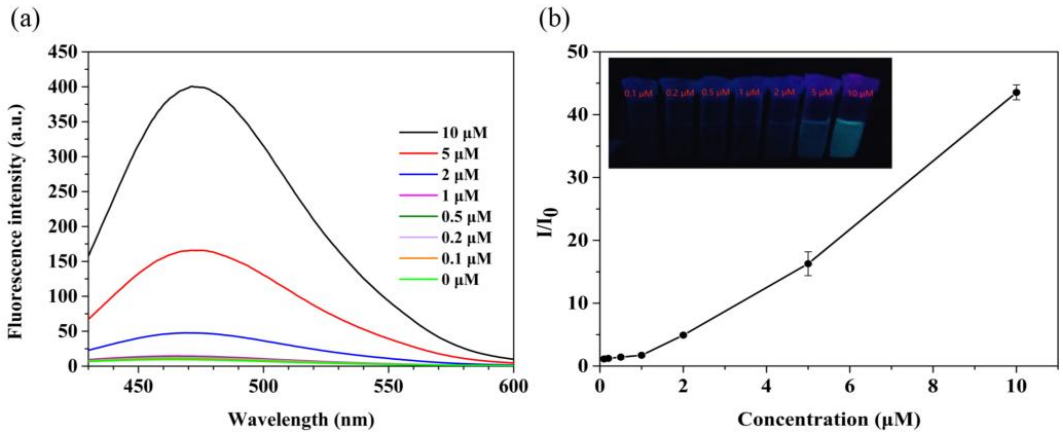

Fig. S9 Concentration-dependent AIE properties of TPE-P9. (a) Emission spectra of TPE-P9 (0-10 μM) in Tris-HCl buffer, λ_{ex} = 330 nm. (b) Plot of fluorescence intensities of emission maximum of TPE-P9 versus its different concentrations in Tris-HCl buffer. I_0 and I are the maximum fluorescence intensity recorded before and after adding dye to the buffer. Inset: photograph of 0.1-10 μM TPE-P9 dissolved in Tris-HCl buffer taken under irradiation with a UV light of 365 nm.

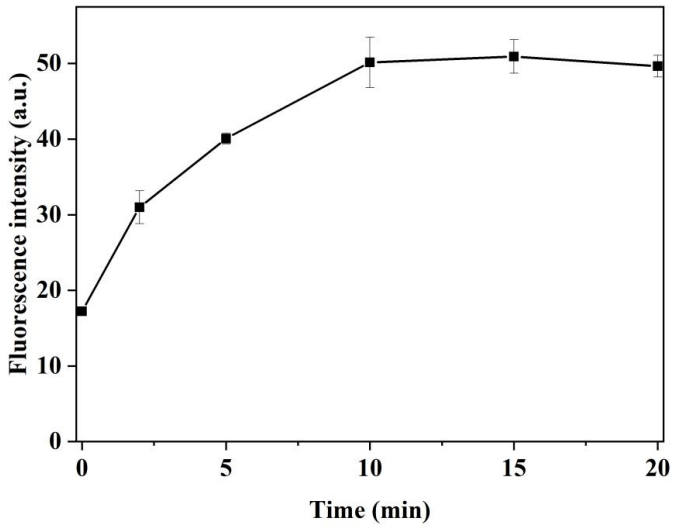

Fig. S10 Time-dependent curve of TPE-P9 (1 μM) toward Tau fibrils (4 μM).

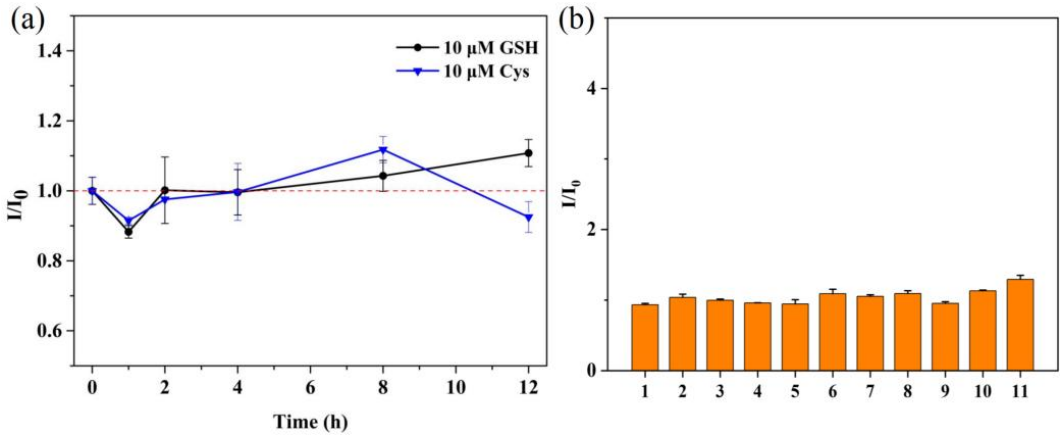

Fig. S11 (a) Fluorescent responses of TPE-P9 (1 μM, λ_{ex} = 330 nm) toward Cys (10 μM) and GSH (10 μM) in Tris-HCl buffer. (b) TPE-P9 (1 μM, λ_{ex} = 330 nm) toward other analytes (10 μM) in Tris-HCl buffer: (1) Al^{3+}; (2) Ca^{2+}; (3) Cu^{2+}; (4) Fe^{2+}; (5) Fe^{3+}; (6) Mg^{2+}; (7) Zn^{2+}; (8) L-Arg; (9) L-Glu; (10) Gly; (11) Met. I_0 and I are the maximum fluorescence intensity recorded before and after adding the analytes to the dye solution.

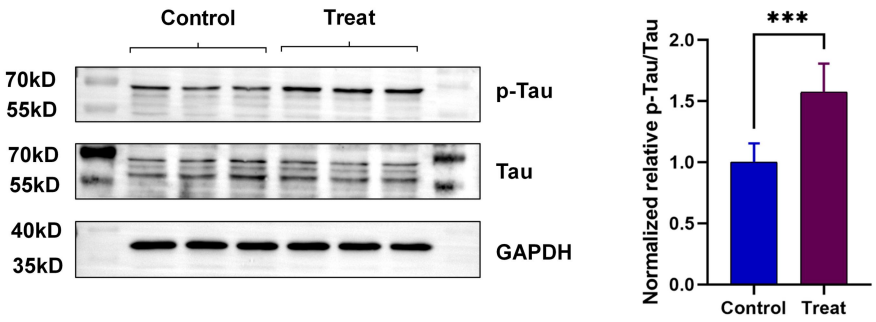

Fig. S12 Western blot analysis of the normalized relative ratio of p-Tau to Tau. After treatment with OA (100 nM) for 12 h, neuronal proteins were visualized with p-Tau, Tau, and GAPDH specific antibodies and their corresponding statistical analysis. Data are means ± SD (n = 6). ***P < 0.001 (unpaired t test).

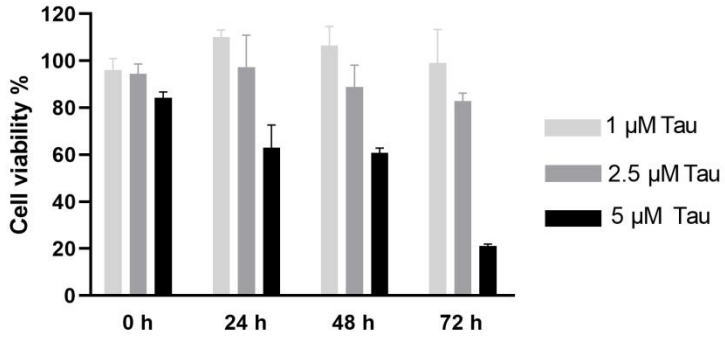

Fig. S13 Viability of HT22 cells after 48 h treatment of 1-5 μM Tau with different GSK3β induced time. Data are means ± SD (n = 3).

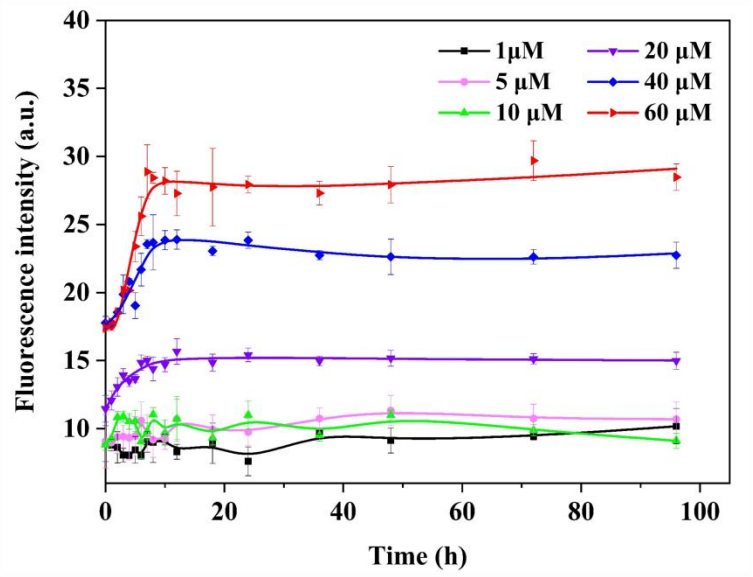

Fig. S14 Time-dependent ThT (10 μM) fluorescence curves to monitor the aggregation kinetics of TPE-P9.

Table S1. Comparison of various tauopathy therapeutics in terms of their action mechanisms

Function	Action mechanism	Compound name	Reference
Inhibiting pathological Tau production	Down-regulating kinase activity	Lithium chloride, hydrogen sulfide	2, 3
	Up-regulating phosphatase activity	Sodium selenate, resveratrol	4, 5
	Blocking pathological Tau aggregation	Cl-NQTrp, rosmarinic acid	6, 7
	Depolymerizing the produced aggregates	NBB BSc3507, GQDs	8, 9
	Blocking pathological Tau aggregation	TPE-P9	This work
	Modulating Tau-HSPGs interaction		
Inhibiting pathological Tau spread	Inhibiting exosomes releasing	GSK1482160, cambinol	10, 11
	Modulating Tau-HSPGs interaction	Tetrasaccharide 27, SN7-13	12, 13
	Blocking micropinocytosis	Cytochalasin D, flubendazole	14, 15

Table S2. Comparison of various amyloid protein detectors and modulators in terms of their specificities, K_D values and relative modulation rates

	Compound name	Target	K_D (μM)	Modulation rate (%)	Reference
Single functional detectors	TPE-Q	Aβ，liquid viscosity	-	-	[16]
	AN-SP, taBODIPY	Aβ，K18-Tau, IAPP	-	-	[17]
	DMNDC	Insulin, α-synuclein	10.6 (insulin)	-	[18]
	Ru-fipc	Aβ	242	-	[19]
	NMM	Aβ	~2.24	-	[20]
Single functional modulators	Cloridarol	hIAPP	-	57	[21]
	TS2	hIAPP	-	~80	[22]
	Bexarotene	Aβ	-	99	[23]
	GAGs	α-Synuclein	-	20-30	[24]
	SC-D	α-Synuclein	-	43	[25]
Dual-functional detectors and modulators	DMA-SLOH	Aβ	4.29	-	[26]
	TPE-P9	Tau	4.46	136	This work

RAW DATA

Fig. 6c

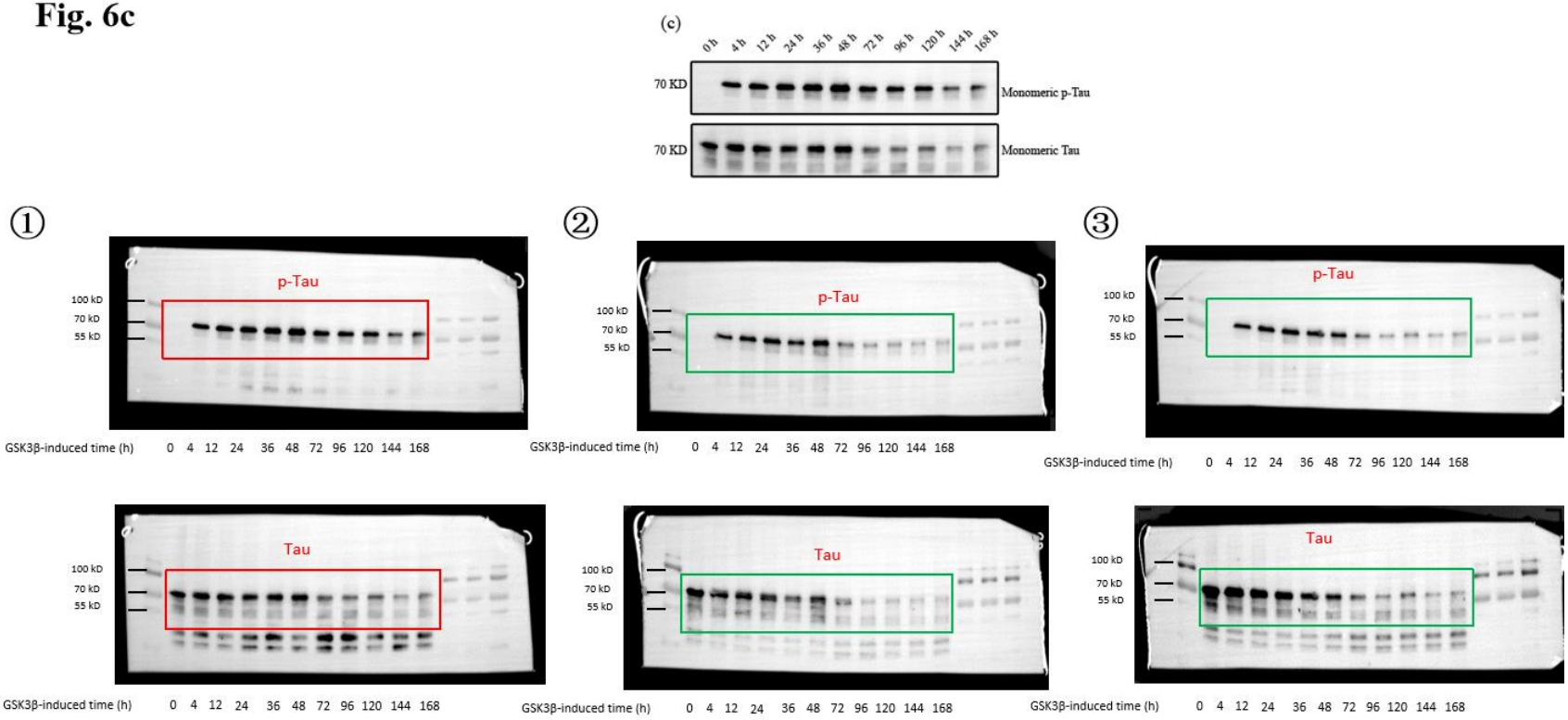

Fig. 6e

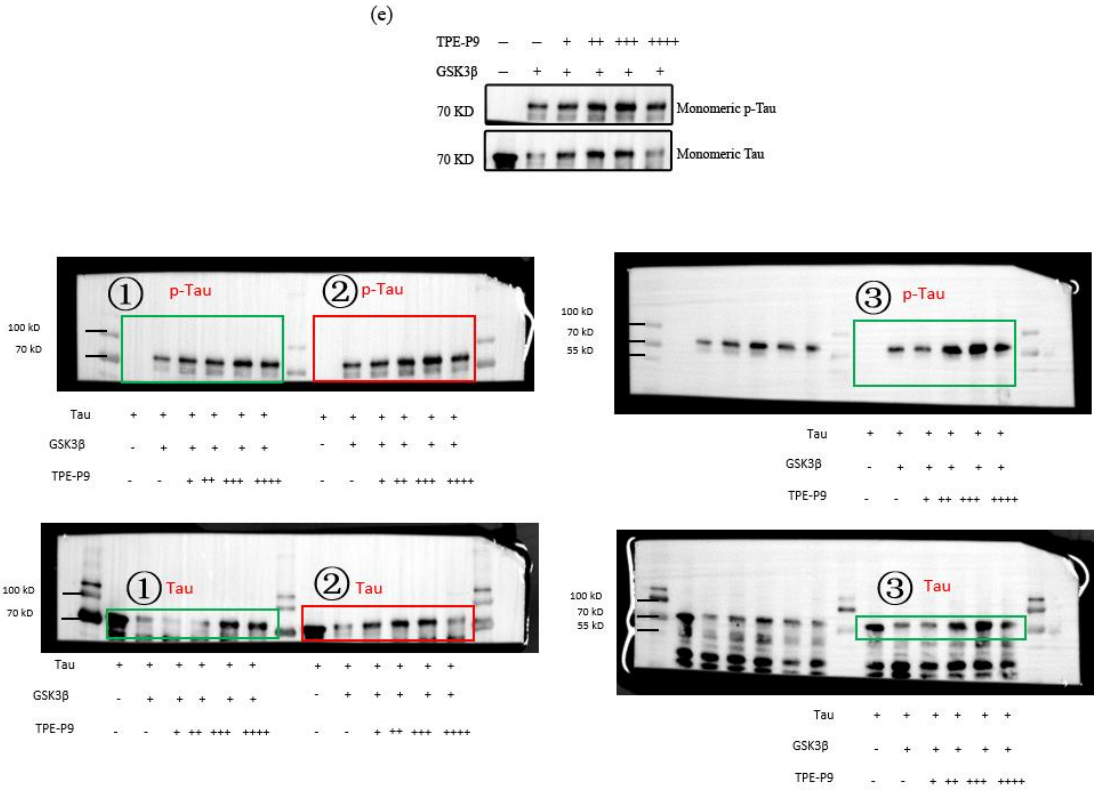
(e)
TPE-P9 – – + ++ +++ ++++
GSK3β – + + + + +
70 KD
Monomeric p-Tau
70 KD
Monomeric Tau
① p-Tau
② p-Tau
100 kD
70 kD
Tau + + + + + + + + + + + +
GSK3β - + + + + + - + + + + +
TPE-P9 - - + ++ +++ ++++ - - + ++ +++ ++++
③ p-Tau
100 kD
70 kD
55 kD
Tau + + + + + +
GSK3β - + + + + +
TPE-P9 - - + ++ +++ ++++
① Tau
② Tau
100 kD
70 kD
Tau + + + + + + + + + + + +
GSK3β - + + + + + - + + + + +
TPE-P9 - - + ++ +++ ++++
③ Tau
100 kD
70 kD
55 kD
Tau + + + + + +
GSK3β - + + + + +
TPE-P9 - - + ++ +++ ++++

Fig. 7c

(c)

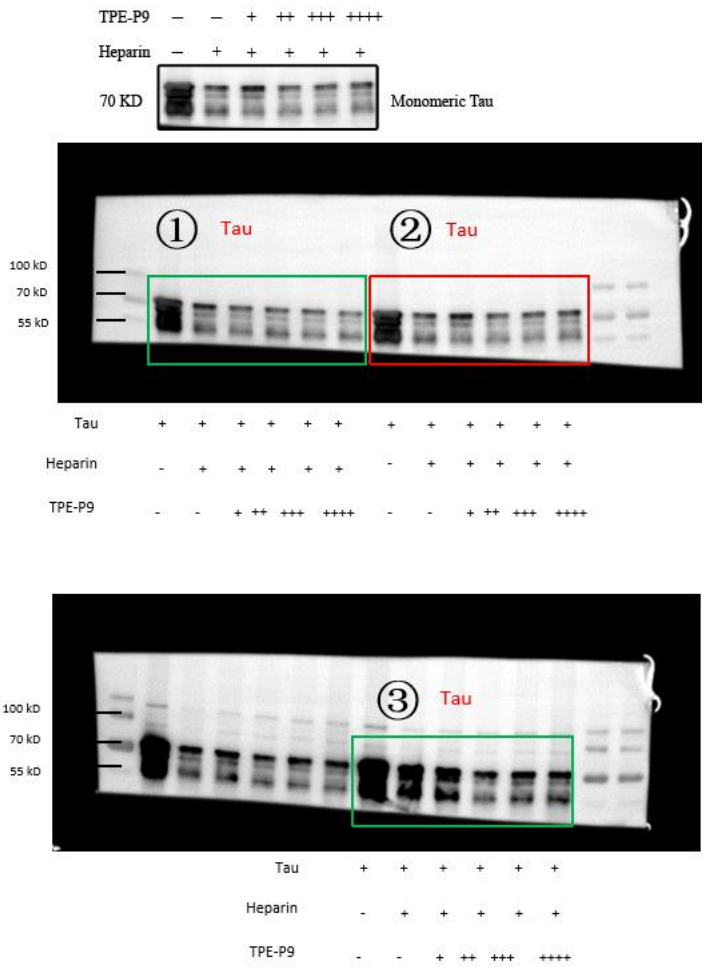
TPE-P9 – – + ++ +++ ++++
Heparin – + + + + +
70 KD
Monomeric Tau
① Tau
② Tau
100 kD
70 kD
55 kD
Tau + + + + + + + + + + + +
Heparin - + + + + + - + + + + +
TPE-P9 - - + ++ +++ ++++ - - + ++ +++ ++++
③ Tau
100 kD
70 kD
55 kD
Tau + + + + + +
Heparin - + + + + +
TPE-P9 - - + ++ +++ ++++

Fig. S12

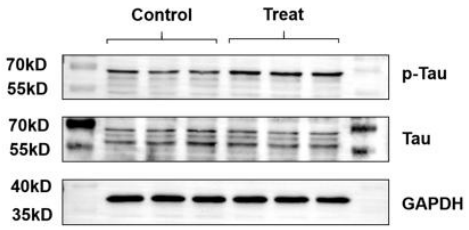

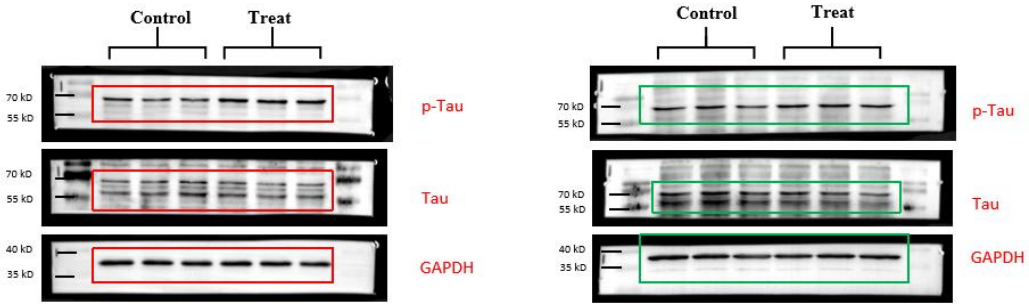

* The bands within the red frame are the unedited original bands corresponding to the bands presented in the manuscript, and the bands within the green frame are the raw data for the replicate experiments.

REFERENCES

1. D. Hu, L. Mao, M. Wang, H. Huang, R. Hu, H. Ma, J. Yuan and Y. Wei, *ACS Appl. Mater. Interfaces*, 2022, **14**, 3485-3495.
2. M. Pérez, F. Hernández, F. Lim, J. Díaz-Nido and J. Avila, *J. Alzheimer's Dis.*, 2003, **5**, 301-308.
3. D. Giovinazzo, B. Bursac, J. I. Sbodio, S. Nalluru, T. Vignane, A. M. Snowman, L. M. Albacarys, T. W. Sedlak, R. Torregrossa, M. Whiteman, M. R. Filipovic, S. H. Snyder and B. D. Paul, *Proc. Natl. Acad. Sci. U.S.A.*, 2021, **118**, e2017225118.
4. J. van Eersel, Y. D. Ke, X. Liu, F. Delerue, J. J. Kril, J. Götz and L. M. Ittner, *Proc. Natl. Acad. Sci. U.S.A.*, 2010, **107**, 13888-13893.
5. S. Schweiger, F. Matthes, K. Posey, E. Kickstein, S. Weber, M. M. Hettich, S. Pfurtscheller, D. Ehninger, R. Schneider and S. Krauß, *Sci. Rep.*, 2017, **7**, 13753-13765.
6. M. Frenkel-Pinter, S. Tal, R. Scherzer-Attali, M. Abu-Hussien, I. Alyagor, T. Eisenbaum, E. Gazit and D. Segal, *Neurodegener. Dis.*, 2017, **17**, 73-82.
7. A. Cornejo, F. Aguilar Sandoval, L. Caballero, L. Machuca, P. Muñoz, J. Caballero, G. Perry, A. Ardiles, C. Areche and F. Melo, *J. Enzym. Inhib. Med. Ch.*, 2017, **32**, 945-953.
8. A. Taghavi, S. Nasir, M. Pickhardt, R. H.-v. Hauβen, G. Mall, E. Mandelkow, E.-M. Mandelkow and B. Schmidt, *J. Alzheimer's Dis.*, 2011, **27**, 835-843.
9. R. Zhu, K. M. Makwana, Y. Zhang, B. H. Rajewski, J. R. Del Valle and Y. Wang, *J. Mater. Chem. B*, 2023, **11**, 7378-7388.
10. Z. Ruan, J.-C. Delpech, S. Venkatesan Kalavai, A. A. Van Enoo, J. Hu, S. Ikezu and T. Ikezu, *Mol. Neurodegener.*, 2020, **15**, 47-60.
11. T. Bilousova, C. Elias, E. Miyoshi, M. P. Alam, C. Zhu, J. Campagna, K. Vadivel, B. Jagodzinska, K. H. Gylys and V. John, *Biochem. Bioph. Res. Co.*, 2018, **499**, 751-757.
12. P. Wang, F. L. Cascio, J. Gao, R. Kayed and X. Huang, *Chem. Comm.*, 2018, **54**, 10120-10123.
13. B. E. Stopschinski, T. L. Thomas, S. Nadji, E. Darvish, L. Fan, B. B. Holmes, A. R. Modi, J. G. Finnell, O. M. Kashmer, S. Estill-Terpack, H. Mirbaha, H. S. Luu and M. I. Diamond, *J. Biol. Chem.*, 2020, **295**, 2974-2983.
14. O. L. Mooren, B. J. Galletta and J. A. Cooper, *Annu. Rev. Biochem.*, 2012, **81**, 661-686.
15. H. P. Lin, B. Singla, P. Ghoshal, J. L. Faulkner, M. Cherian‐Shaw, P. M. O'Connor, J. X. She, E. J. Belin de Chantemele and G. Csányi, *Brit. J. Pharmacol.*, 2018, **175**, 3640-3655.
16. H. Yao, N. Wang, Y. Shi, S. Fang, M. Wu, H. Fan, Y. Zhang, H. Chong, T. Wang, H. Li and C. Wang, *New J. Chem.*, 2023, **47**, 2932-2941.
17. Y. Li, S. Awasthi, L. Bryan, R. S. Ehrlich, N. Tonali, S. Balog, J. Yang, N. Sewald and M. Mayer, *ACS Chem. Neurosci.*, 2024, **15**, 3113-3123.
18. A. Das, T. Dutta, L. Gadhe, A. L. Koner and I. Saraogi, *Anal. Chem.*, 2020, **92**, 10336-10341.
19. H.-j. Yu, W. Zhao, M. Xie, X. Li, M. Sun, J. He, L. Wang and L. Yu, *Anal. Chem.*, 2020, **92**, 2953-2960.
20. M. Li, A. Zhao, J. Ren and X. Qu, *ACS Chem. Neurosci.*, 2017, **8**, 1299-1304.
21. Y. Tang, Y. Liu, Y. Zhang, D. Zhang, X. Gong and J. Zheng, *ACS Chem. Neurosci.*, 2021, **12**, 1419-1427.
22. B. Ren, Y. Liu, Y. Zhang, M. Zhang, Y. Sun, G. Liang, J. Xu and J. Zheng, *J. Mater. Chem. B*, 2018, **6**, 56-67.
23. J. Habchi, P. Arosio, M. Perni, A. R. Costa, M. Yagi-Utsumi, P. Joshi, S. Chia, S. I. A. Cohen, M. B. D. Müller, S. Linse, E. A. A. Nollen, C. M. Dobson, T. P. J. Knowles and M. Vendruscolo, *Sci. Adv.*, 2016, **2**, e1501244.
24. S. Mehra, D. Ghosh, R. Kumar, M. Mondal, L. G. Gadhe, S. Das, A. Anoop, N. N. Jha, R. S. Jacob, D. Chatterjee, S. Ray, N. Singh, A. Kumar and S. K. Maji, *J. Biol. Chem.*, 2018, **293**, 12975-12991.
25. J. Pujols, S. Peña-Díaz, D. F. Lázaro, F. Peccati, F. Pinheiro, D. González, A. Carija, S. Navarro, M. Conde-Giménez, J. García, S. Guardiola, E. Giralt, X. Salvatella, J. Sancho, M. Sodupe, T. F. Outeiro, E. Dalfó and S. Ventura, *P. Natl. Acad. Sci.*, 2018, **115**, 10481-10486.
26. Y. Li, D. Xu, S.-L. Ho, H.-W. Li, R. Yang and M. S. Wong, *Biomaterials*, 2016, **94**, 84-92.